Journal of Statistical Mechanics: Theory and Experiment
An IOP and SISSA journal

On the efficiency of the equation-free closure of statistical moments: dynamical properties of a stochastic epidemic model on Erdős–Rényi networks

A I Reppas[1,3], Y De Decker[2] and C I Siettos[1,4]

[1] School of Applied Mathematics and Physical Sciences, National Technical University of Athens, Greece
[2] Center for Nonlinear Phenomena and Complex Systems, Université Libre de Bruxelles, Belgium
E-mail: areppas@mpi-inf.mpg.de, ydedecke@ulb.ac.be and ksiet@mail.ntua.gr

Received 10 May 2012
Accepted 9 August 2012
Published 31 August 2012

Online at stacks.iop.org/JSTAT/2012/P08020
doi:10.1088/1742-5468/2012/08/P08020

Abstract. We show how different explicit statistical moment closures, including the mean field and the Kirkwood approximations as well as an Ursell-type expansion for the moments, compare with the equation-free approach in the case of a stochastic epidemic model evolving on Erdős–Rényi networks. For illustration purposes we use a simple, discrete susceptible–infected–recovered stochastic model with a nonlinear recovering probability. For every closure scheme, we derive the corresponding macroscopic evolution equations and we construct the bifurcation diagrams with respect to the probability of infection. Finally, we construct the coarse-grained bifurcation diagram obtained with the equation-free method acting directly on the microscopic simulations, bypassing the derivation of explicit closures. We show that the equation-free approach captures the actual emergent nonlinear behavior and outperforms all the other explicit schemes.

[3] Present address: Department of Computational Biology and Applied Algorithmics, Max-Planck-Institut für Informatik, Campus E1 4, 66123 Saarbrücken, Germany.
[4] Author to whom any correspondence should be addressed.

1742-5468/12/P08020+24$33.00

J. Stat. Mech. (2012) P08020

Keywords: random graphs, networks, nonlinear dynamics, stochastic processes, epidemic modelling

Contents

1. Introduction

Over recent years, individual-based and dynamic network-agent-based models have been regarded as key state-of-the-art approaches for reasoning about (and analyzing) complex epidemic systems [1]–[4]. They are indeed built upon the best available agent level, local type of information such as the individual recovery time, host–pathogen interactions, host–host connectivity, etc.

But while these models are now becoming the backbone of current modeling practice, they intrinsically suffer from a major drawback due to the intrinsic multiplicity of the scales at which the relevant dynamics evolve. Notwithstanding the level of accuracy of the local level of description, the relevant information is typically found at a much larger, macroscopic scale. It is indeed the behavior of the system as a whole, the *collective* dynamics that underlies systematic epidemiological analyses, such as the prediction of disease propagation in space and time or the devise of optimal vaccination or control policies. One then typically faces the daunting task of extracting macro-scale dynamics (at the level of a region, city, country, or the globe) from micro-scale evolution rules (micro/molecular, host or pathogen description).

The increasing complexity of epidemic models makes the accurate modeling and analysis of the emergent dynamics at the macroscopic level an overwhelmingly difficult

J. Stat. Mech. (2012) P08020

task. A first way to analyze the emergent dynamics is to run simple 'brute force' simulations of the detailed agent-based model. A simple simulation would be carried out as follows: many initial conditions would be set up; a large enough number of realizations would be created for each initial condition; some of the rules would probably have to be changed before running the detailed dynamics of the system for a long time to investigate how parameters such as vaccination policies or virus pathogenicity may influence the spread of an outbreak. However, such simulations typically 'live' on extremely fine space and time scales, and simple simulation is insufficient for the systematic analysis, design and optimization of epidemic systems. In addition, testing many different scenarios and realizations is also time-demanding, even prohibitive. That situation worsens as the complexity of the detailed model increases.

Another approach consists in extracting evolution laws for a few selected collective (coarse-grained) variables and analyzing their dynamics with the best available analytical or computational techniques. There indeed exists an arsenal of numerical techniques geared towards ordinary and/or partial (integro) differential equations, such as integration packages or continuation-based bifurcation analyses [5]–[7]. The difficulty here resides in the extraction of the macroscopic evolution laws themselves. The stochastic dynamics of the simulations can be described by a master equation (these processes are typically Markovian) from which evolution equations can be obtained for the desired moments of the underlying probability distribution (in general, low-order moments such as the average infected population). However, these equations usually involve higher-order moments whose evolution laws themselves comprise even higher order moments, leading to an infinite hierarchy of evolution equations. To overcome this problem, various *closure* approximation methods have been proposed. They typically relate higher-order moments to a few, low-order ones.

The simplest closure consists in expressing the emergent dynamics only in terms of the averages, by neglecting all (cross)-correlations between the involved stochastic variables. While appealing due to its simplicity, this approach often fails in predicting, even qualitatively, the dynamics of simulations on networks. More sophisticated approaches have thus been developed. One of the most popular higher-order approximations is the so-called *pair-wise approximation scheme* which relates third-order moments (that would here correspond to the averaged triplets of states of individuals) with second moments (averaged pairs of individuals) [8]–[10]. Other approaches have been and still are proposed, as can be seen in the recent literature. Simon *et al* [11] derived an exact formulation of a simple Susceptible–Infected–Susceptible (SIS) epidemic model evolving on an arbitrary network using a continuous Markov chain process, revealing its relevance to pair-wise moment closures. Keeling and Ross [12] derived the Kolmogorov's forward equations for Markov epidemic processes in order to approximate the emergent dynamics of small populations. Taylor *et al* [13] formalized the link between a pair-wise approximation and the Markovian representation for a SIS model. Hausken and Moxnes [14] presented a closure scheme named covariance closure based on the Dirac distribution, allowing the derivation of higher-order approximations. Murrel *et al* [15] derived power-1, power-2 and power-3 spatial moment closures to approximate population dynamics in continuous space. Bauch [16] proposed an alternative second-order moment closure scheme for epidemic dynamics on regular lattices. Filipe and Gibson [17] presented a square-wise approximation which is a third-order closure and compared its performance to mean field and pair-wise

J. Stat. Mech. (2012) P08020

approximations in the context of a SIS model. Hiebeler [18] investigated the completeness of power-1, power-2 and power-3 closure schemes presented in [15] and Brown and Bolker [19] compared the efficiency of such closures for a household SIS epidemic model. Rogers [20] presented a maximum-entropy moment closure scheme for stochastic systems evolving on networks and compared it with pair-wise approximations in the context of a susceptible–infected–recovering (SIR) model on a square regular lattice.

While these approaches offer a good starting point for analyzing (network) epidemic dynamics in a more systematic way, they still impose more or less some bias (e.g. assumptions of infinite size population, homogeneous agents, homogeneous or regular networks) and therefore may miss important quantitative and/or qualitative information at the coarse-grained level. This situation worsens again as the interaction dynamics becomes more complex (see for example the critical discussion in [21]). Over the past few years it has been demonstrated that the *equation-free* approach [22]–[28] can establish in a different way a bridge between traditional numerical analysis and microscopic/stochastic simulation. Equation-free analysis is a system-identification-based computational approach that sidesteps the necessity of deriving good 'explicit' closures: they are instead obtained 'on-the-fly' by running appropriately conditioned microscopic simulations of the detailed model. One is then able to estimate the same information as a continuum model would do from an explicit formula, but now bypassing the need of analytical derivation of macroscopic-level equations. Using this framework, continuation and numerical bifurcation analysis, including stability computations of the complex-emergent macroscopic dynamics, can be performed in a fully computational manner.

In this work, we assess the efficiency of the equation-free computational approach with respect to various explicit closure approximation schemes, in the case of epidemic models evolving on complex networks. More specifically, using a simple susceptible–infected–recovering–susceptible (SIRS) stochastic model evolving on an Erdős–Rényi network we construct the bifurcation diagram with respect to the probability of disease transmission. We compare the diagram obtained from direct ('brute force') simulations to those obtained with the mean field approximation, with a pair-level approximation (the Kirkwood factorization [29]), a second-order Ursell moment expansion scheme [30], a 'Bethe-type' ansatz [31, 32] and finally with the equation-free approach. We show that the proposed schemes approximate qualitatively the actual emergent dynamics. However, it is demonstrated that the equation-free approach captures in an exact quantitative manner the actual emergent behavior, outperforming all other explicit schemes. We also discuss the reasons behind the efficiency of this approach in our case and the applicability and relevance of this technique for other discrete stochastic models.

2. The individual-based stochastic epidemic model

Our illustrative model consists of a population of N individuals who interact through a caricature of a social network, which in our case is approximated by an Erdős–Rényi distributed network in which each node is connected with the other $N-1$ nodes with a probability p [33]. The degree distribution follows the binomial law:

$$P(k) = \binom{N-1}{k} p^k (1-p)^{N-1-k} \tag{1}$$

J. Stat. Mech. (2012) P08020

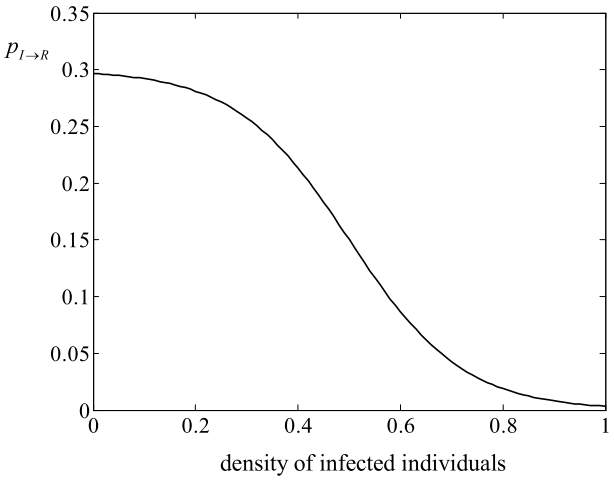

Figure 1. The probability of recovery as a function of the density of the infected individuals.

This distribution is symmetric around the mean value $\bar{k} = pN$. In our case we used a population of $N = 10\,000$, while the probability parameter of the Erdős–Rényi network was set to $p = 0.0008$, resulting in a network with a mean distributed connectivity degree of about 8.

In the model, each individual can be in one of the following three states: susceptible (S), infected (I) or recovered (R). The states of the individuals change at every discrete time step in a probabilistic way, according to the following simple rules involving their own states and the states of their links:

- Rule #1: an infected individual (I) infects a susceptible (S) neighbor with a probability $p_{S\to I} = \lambda$ if an active link exists between them.
- Rule #2: an infected individual (I) recovers with a probability $p_{I\to R} = \delta$. In our model, the probability of recovery depends nonlinearly, at each time step, on the overall density of infected individuals $[I] = N_I/N$. Here, this dependence is given by the following function

$$\delta = 0.3\left(1 - \frac{1}{1 + \exp^{-9([I]-0.5)}}\right)$$

  as depicted in figure 1.
- Rule#3: a recovered individual (R) becomes susceptible (S) with a probability $p_{R\to S} = \gamma$. This condition expresses the case of temporal immunity. In the case we studied we used $\gamma = 1/5$.

The above rules define a complex stochastic model that will change the state of each individual as a function of time. As mentioned earlier, one is however typically interested in the analysis of the dynamics at the macroscopic (emergent) level. One of the possibilities to do so consists in extracting the time evolution of a few selected moments of the underlying distribution probability from the stochastic dynamics. Let us introduce $P_t(a_x)$, denoting the probability of node x to be in the state a $(=S, I, R)$ at time t. The evolution of these

single-site probabilities for the epidemic model under consideration is expressed as [34, 35]:

$$\begin{aligned}
\frac{\mathrm{d}P_t(S_x)}{\mathrm{d}t} &= -\lambda \sum_{y\in N(x)} P_t(S_x, I_y) + \gamma P_t(R_x) \\
\frac{\mathrm{d}P_t(I_x)}{\mathrm{d}t} &= \lambda \sum_{y\in N(x)} P_t(S_x, I_y) - \delta P_t(I_x) \\
\frac{\mathrm{d}P_t(R_x)}{\mathrm{d}t} &= \delta P_t(I_x) - \gamma P_t(R_x)
\end{aligned} \tag{2}$$

where $N(x)$ is the neighborhood of node x and $P_t(a_x, b_y)$ is the joint probability of node x to be in the state a and its neighbor y to be in the state b at time t. It should be also emphasized that, at each time step, one has $P_t(S_x) + P_t(I_x) + P_t(R_x) = 1$.

These evolution equations involve second-order moments, the evolution equations of which can be deduced from the transition rules of the epidemic model:

- The pair $(R_x, I_y) \to (S_x, I_y)$ with a rate γ
- The pair $(S_x, I_y) \to (I_x, I_y)$ with a rate λ
- The pair $(S_x, I_y) \to (S_x, R_y)$ with a rate δ
- The triplet $(S_x, S_y, I_w) \to (S_x, I_y, I_w)$ with a rate λ
- The triplet $(I_x, S_y, I_w) \to (I_x, I_y, I_w)$ with a rate λ.

This leads to

$$\begin{aligned}
\frac{\mathrm{d}P_t(S_x, I_y)}{\mathrm{d}t} &= \gamma P_t(R_x, I_y) - (\lambda + \delta) P_t(S_x, I_y) \\
&\quad + \sum_{w\in N^x(y)} \lambda P_t(S_x, S_y, I_w) - \sum_{w\in N^y(x)} \lambda P_t(I_w, S_x, I_y) \\
\frac{\mathrm{d}P_t(S_x, R_y)}{\mathrm{d}t} &= \delta P_t(S_x, I_y) + \gamma P_t(R_x, R_y) \\
&\quad - \gamma P_t(S_x, R_y) - \sum_{w\in N^y(x)} \lambda P_t(I_w, S_x, R_y) \\
\frac{\mathrm{d}P_t(R_x, I_y)}{\mathrm{d}t} &= -(\gamma + 1) P_t(R_x, I_y) + \delta P_t(I_x, I_y) \\
&\quad + \sum_{w\in N^y(x)} \lambda P_t(R_x, S_y, I_w)
\end{aligned} \tag{3}$$

where $P_t(a_x, b_y, c_w)$ is now the joint probability for node x to be in state a, one of its neighbors y to be in state b and another neighbor w to be at state c at time t (see figure 2). $N^x(y)$ denotes the neighbors of node y from which we have excluded node x. Note that all the pair probabilities are not present here, but can be obtained using conservation rules such as

$$\begin{aligned}
P_t(S_x, S_y) + P_t(S_x, I_y) + P_t(S_x, R_y) &= P_t(S_x) \\
P_t(I_x, S_y) + P_t(I_x, I_y) + P_t(I_x, R_y) &= P_t(I_x) \\
P_t(R_x, S_y) + P_t(R_x, I_y) + P_t(R_x, R_y) &= P_t(R_x).
\end{aligned} \tag{4}$$

The system of equations (2) and (3) is not a closed system as we have the presence of probabilities of triplets. In order to derive a set of autonomous equations for the moments,

J. Stat. Mech. (2012) P08020

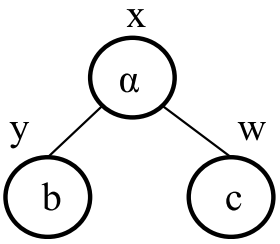

Figure 2. The case where a node x is in state a and its neighbors are in states b and c respectively.

one has to 'close' the above kinetic laws. This is most often done by expressing higher-order moments as functionals of the lower ones. In section 3, we thus present several ways to do so that lead to different effective reduced dynamical systems.

3. Explicit closure of the evolution equations for the moments

In this section, we present different approximation (closure) schemes for the evolution laws described above. Generally speaking, these approximations are based on some assumptions made on the importance and/or type of correlations existing between the individuals of the network. Let us analyze them in detail.

3.1. Mean field description

The simplest level of description is based on a series of approximations typically referred to as 'mean field' hypothesis. It consists in factorizing pair and triplet probabilities directly in terms of the local occupation probabilities, so that

$$\begin{aligned} P_t(a_x, b_y) &= P_t(a_x)P_t(b_y) \\ P_t(a_x, b_y, c_w) &= P_t(a_x)P_t(b_y)P_t(c_w). \end{aligned} \tag{5}$$

These relations imply the absence of any statistical correlation between neighboring nodes. Assuming from now on that our system is homogeneous, we take node x as an origin and define [34]:

$$[ab] = \frac{1}{z}\sum_{y\in N(x)} P_t(a_x, b_y); \qquad z = \bar{k} = 8. \tag{6}$$

One then readily obtains the evolution equations for the spatially averaged densities of node states. These evolution equations read

$$\begin{aligned} \frac{\mathrm{d}[S]}{\mathrm{d}t} &= -\lambda z[S][I] - \gamma(1 - [S] - [I]) \\ \frac{\mathrm{d}[I]}{\mathrm{d}t} &= \lambda z[S][I] - \delta[I] \end{aligned} \tag{7}$$

given that

$$[R] = 1 - [S] - [I].$$

Although quite simple, this approximation is often not efficient as it generally describes very poorly the dynamics of simulations. A higher level of description is typically needed, such as the Kirkwood factorization.

3.2. Kirkwood factorization

The so-called Kirkwood superposition approximation (or factorization) consists in a simple closure expression that connects the triplet probabilities to the doublet and singlet probabilities:

$$P_t(a_x, b_y, c_w) = \frac{P_t(a_x, b_y)P_t(b_y, c_w)P_t(a_x, c_w)}{P_t(a_x)P_t(b_y)P_t(c_w)}. \tag{8}$$

This factorization seems to have been first introduced by Kirkwood to estimate the 3-point correlation function appearing when one tries to characterize the radial distribution function of a liquid [29]. It has been widely used to assess the properties of liquids, but also has become very popular in the closure of chemical kinetic equations for surface reactions (see [36] for one of the earliest examples). It is typically combined with an approximation on the Markovianity (in space) of the underlying stochastic processes, so that $P_t(a_x, c_w) = P_t(a_x)P_t(c_w)$ and hence

$$P_t(a_x, b_y, c_w) = \frac{P_t(a_x, b_y)P_t(b_y, c_w)}{P_t(b_y)}. \tag{9}$$

Using this approximation the systems of equations (2) and (3) can now be 'closed' in terms of the previously introduced average occupation states and densities of pairs and triplets of nodes, given that

$$[abc] = \frac{1}{z-1} \sum_{w \in N^x(y)} P_t(a_x, b_y, c_w). \tag{10}$$

Using these, the system (2) and (3) now becomes

$$\begin{aligned}
\frac{\mathrm{d}[I]}{\mathrm{d}t} &= \lambda z[SI] - \delta[I] \\
\frac{\mathrm{d}[R]}{\mathrm{d}t} &= \delta[I] - \gamma[R] \\
\frac{\mathrm{d}[SR]}{\mathrm{d}t} &= \delta[SI] + \gamma([R] - [RI] - 2[SR]) - \frac{(z-1)\lambda[SI][SR]}{1-[R]-[I]} \\
\frac{\mathrm{d}[RI]}{\mathrm{d}t} &= -(2\delta+\gamma)[RI] + \delta([I] - [SI]) + \frac{(z-1)\lambda[SI][SR]}{1-[R]-[I]} \\
\frac{\mathrm{d}[SI]}{\mathrm{d}t} &= \gamma[RI] - (\lambda+\delta)[SI] + \frac{(z-1)\lambda[SI]}{1-[R]-[I]}(1-[R]-[I]-[SR]-2[SI])
\end{aligned} \tag{11}$$

where

$$[SS] + [SR] + [SI] = [S] \qquad [RS] + [RI] + [RR] = [R].$$

The system (11) forms the evolution equations for the first two moments of the underlying stochastic variables under the Kirkwood approximation scheme.

J. Stat. Mech. (2012) P08020

3.3. Ursell expansion

The Kirkwood approximation is not the only closure scheme that builds on assumptions made on the extent of spatial correlations. Different closures can also be obtained starting from an approach based on an Ursell-type expansion, in which a systematic development of the n-plets probabilities is done in terms of spatial correlation functions. In our case, this expansion would look like

$$\begin{aligned} P_t(a_x, b_y) &= P_t(a_x)P_t(b_y) + f_{a_x b_y} \\ P_t(a_x, b_y, c_w) &= P_t(a_x)P_t(b_y)P_t(c_w) + P_t(a_x)f_{b_y c_w} + P_t(b_y)f_{a_x c_w} \\ &\quad + P_t(c_w)f_{a_x b_y} + f_{a_x b_y c_w} \\ &\quad \dots \end{aligned} \tag{12}$$

and so forth for higher-order moments. The advantage of this expansion is that it introduces explicitly the same-time two-point correlation functions f_{ij} as well as three-point correlation functions f_{ijk}. From there, one can use different hypotheses. A popular one assumes that the three-points correlation functions are very small, and that two-point correlations become negligible for nodes which are not first neighbors, so that $f_{a_x c_w}$ is also zero. This leads to

$$P_t(a_x, b_y, c_w) = P_t(a_x)P_t(b_y, c_w) + P_t(c_w)P_t(a_x, b_y) - P_t(a_x)P_t(b_y)P_t(c_w). \tag{13}$$

This procedure can be extended systematically to longer-range correlations, but usually involves only pair correlation functions (see for example [30]). In order to decide where to stop the expansion, one can follow the time evolution of correlations from simulations and deduce which ones should be retained or not.

This closure allows the expression of the evolution equations (2) and (3) in terms of singlet and doublet probabilities only, using

$$\begin{aligned} P_t(S_x, S_y, I_w) &= P_t(S_x)P_t(S_y, I_w) + P_t(I_w)P_t(S_x, S_y) - P_t(S_x)P_t(S_y)P_t(I_w) \\ P_t(I_w, S_x, I_y) &= 2P_t(I_w)P_t(S_x, I_y) - P_t(I_w)P_t(S_x)P_t(I_y) \\ P_t(I_w, S_x, R_y) &= P_t(R_x, S_y, I_w) = P_t(I_w)P_t(S_x, R_y) + P_t(R_y)P_t(I_w, S_x) \\ &\quad - P_t(I_w)P_t(S_x)P_t(R_y) \end{aligned} \tag{14}$$

and following the same procedure as the one used for the Kirkwood factorization. It should be noted that, from the point of the view of this expansion approach, the above Kirkwood approximation actually corresponds to some (intricate) factorization of the three-point correlation functions in terms of the two-point ones and the averages. The evolution equations are given in the appendix.

3.4. Bethe-type Ansatz

Another way to closing the evolution equations is to use directly the transition probabilities themselves [31, 32]. To exemplify this approach, consider the occupation numbers S_x, I_x and R_x that are equal to 1 if the site x is susceptible, infected or recovered, respectively and which are zero otherwise. Note that their sum is always equal to one. Let us take a simple example of transition: A susceptible individual located at node x can become infected with probability λ. This corresponds to the transition $S_x \to I_x$ with a probability per unit time $W_x = \lambda S_x I_y$. The first level of Bethe-type ansatz consists in considering that any occupation besides the site itself can be replaced by its ensemble

J. Stat. Mech. (2012) P08020

average, so that now $W_x = \lambda S_x P_t(I_y)$. The physical picture of this is that the node x 'sees' the rest of the system as a bath, a field acting on x. This supposes the total absence of correlation between the site and the rest of the system—in other words, the mean field approximation. It can easily be checked that, indeed, using such transition probabilities per unit time gives rise to the mean field kinetics, because $P_t(W_x) = \lambda P_t(S_x)P_t(I_y)$.

One can however extend this theory further by considering that the basic block is not a site, but a pair of sites (a link). Using this approach, one recovers the evolution equations (2) for the first moments, in which pair probabilities appear explicitly. In deriving the evolution equations for the pair probabilities from the master equation, one will however have to evaluate for, say, $(\mathrm{d}/\mathrm{d}t)P_t(S_x, I_y)$, the quantity $P_t(S_x W_y)$. If one retains the pair probability in the transition probability per unit time, but averages over all the other quantities, this leads to $P_t(S_x W_y) = P_t(S_x)\lambda P_t(S_y, I_w)$. In this way, one closes the system since the triplet probability appearing in the original equation is replaced by a product of singlet and pair probabilities. Similarly, the other triplet in this equation will be factorized as $P_t(I_y)\lambda P_t(I_w, S_x)$. To summarize, the evolution equations (2) and (3) are closed by the following factorization:

$$\begin{aligned} P_t(S_x, S_y, I_w) &= P_t(S_x)P_t(S_y, I_w) \\ P_t(I_w, S_x, I_y) &= P_t(I_y)P_t(I_w, S_x) \\ P_t(I_w, S_x, R_y) &= P_t(R_y)P_t(I_w, S_x) \\ P_t(R_x, S_y, I_w) &= P_t(R_x)P_t(S_y, I_w). \end{aligned} \tag{15}$$

This approximation has often been quite successful in the modeling of lattice dynamics, but is not as well known as the Kirkwood or Ursell approaches. Its success obviously rests on the fact that it is also an approximation for the correlation functions. The evolution equations derived under this approximation are given in the appendix.

4. The equation-free approach for on-demand derivation of closures

The equation-free approach [23] represents a new, alternative way to extract and analyze the collective (emergent) behavior of complex systems directly from the fine, individual level of description. The basic assumption in this approach is that the dynamics of the system can be described by a few macroscopic variables only, but the explicit macroscopic evolution equations are not available in a closed form. Properly performed simulations can be used to efficiently extract 'systems-level' information from the detailed models, bypassing the need for obtaining analytical approximations, providing thus an 'on-demand' model reduction.

Let us first formalize these ideas in a general setting. A detailed computational model takes as an input a detailed state distribution, say $\boldsymbol{U}_0 \equiv \boldsymbol{U}(t_0) \in \Re^N, N \gg 1$ at an arbitrary time t_0, and outputs the values of the state distribution according to some evolution rules after a time interval T, i.e.:

$$\boldsymbol{U}_T = \wp_T(\boldsymbol{U}_0, \boldsymbol{p}) \tag{16}$$

where $\wp_T : \Re^N \times \Re^m \to \Re^N$ is the time-evolution operator, and $\boldsymbol{p} \in \Re^m$ is the vector of system parameters. The key assumption of the approach is that the macroscopic, emergent dynamics of the above-detailed system can be described by a set of continuum level equations, but that the closures that are required to write them in a closed form

J. Stat. Mech. (2012) P08020

are not explicitly available. Let us denote by $\boldsymbol{x} = [x^1, x^2, \ldots, x^n] \in \Re^n, n \ll N$ the set of macroscopic variables that are used to describe the observed aggregate dynamics. Usually, these variables are a few low-order moments of the detailed evolving distributions. The existence of such a macroscopic model implies that the higher-order moments, say, $\mathbf{y} \in \Re^{N-n}$, of the detailed distribution $\mathbf{U}$ become relatively fast functionals of $\boldsymbol{x}$. This *separation of time scales* can be represented in the form of a singularly perturbed system:

$$\frac{\mathrm{d}\boldsymbol{x}(t)}{\mathrm{d}t} = \boldsymbol{f}(\boldsymbol{x}, \boldsymbol{y}, \boldsymbol{p}), \qquad \boldsymbol{x}(t=0) = \boldsymbol{x}_0 \tag{17a}$$

$$\epsilon \frac{\mathrm{d}\boldsymbol{y}(t)}{\mathrm{d}t} = \boldsymbol{g}(\boldsymbol{x}, \boldsymbol{y}, \boldsymbol{p}), \qquad \boldsymbol{y}(t=0) = \boldsymbol{y}_0 \tag{17b}$$

where ϵ is a small positive parameter, i.e. $\epsilon \ll 1$. Equation (17*a*) corresponds to the 'slow' coarse-grained dynamics and equation (17*b*) to the 'fast' dynamics. It has been shown [37] that under certain conditions the overall dynamics of (17) can be approximated within a small time interval by the dynamics of the system

$$\frac{\mathrm{d}\boldsymbol{x}(t)}{\mathrm{d}t} = \boldsymbol{f}(\boldsymbol{x}, \boldsymbol{y}, \boldsymbol{p}) \tag{18a}$$

$$0 = \boldsymbol{g}(\boldsymbol{x}, \boldsymbol{y}, \boldsymbol{p}). \tag{18b}$$

By applying the implicit function theorem, the above system of equations can in turn be written in the form of [37]:

$$\frac{\mathrm{d}\boldsymbol{x}(t)}{\mathrm{d}t} = \boldsymbol{F}(\boldsymbol{x}, \boldsymbol{p}) \tag{19a}$$

$$\text{where } \boldsymbol{F}(\boldsymbol{x}, \boldsymbol{p}) \equiv \boldsymbol{f}(\boldsymbol{x}, \boldsymbol{q}(\boldsymbol{x}, \boldsymbol{p}), \boldsymbol{p}). \tag{19b}$$

$\boldsymbol{q}$ denotes a smooth continuous function defining the relation between the slow and the fast variables after a short (in the macroscopic sense) time interval. The closure

$$\boldsymbol{y} = \boldsymbol{q}(\boldsymbol{x}, \boldsymbol{p}) \tag{20}$$

defines the slow manifold on which the coarse-grained dynamics of the system evolve after a fast macroscopic transient phase.

The equation-free approach provides such a closure *on demand*. This is achieved by appropriately designed short calls of the fine scale simulator (refer to [23] for more detailed discussions). In a nutshell, once the appropriate macroscopic observables have been identified, the procedure reads as follows (figure 3):

(a) Prescribe the coarse-grained initial condition $\boldsymbol{x}(t_0) \equiv \boldsymbol{x}_0$. In the case under consideration, this initial condition would be a set of prescribed densities of infected, susceptible and recovered individuals.

(b) Transform it through a *lifting* operator μ to consistent realizations, which here correspond to a distribution of local states over the network: $\boldsymbol{U}(t_0) = \mu \boldsymbol{x}(t_0)$.

(c) Evolve these detailed realizations in time using the stochastic simulator for a short macroscopic time T, generating $\boldsymbol{U}(t_0 + T)$. The choice of T is associated with the (estimated) spectral gap of the linearization of the unavailable closed macroscopic equations.

(d) Obtain the coarse-grained variables using a restriction operator M: $\boldsymbol{x}_{k+1} \equiv \boldsymbol{x}(t_0 + T) = M\boldsymbol{U}(t_0 + T)$. Here, that step would simply consist in re-estimating the densities.

J. Stat. Mech. (2012) P08020

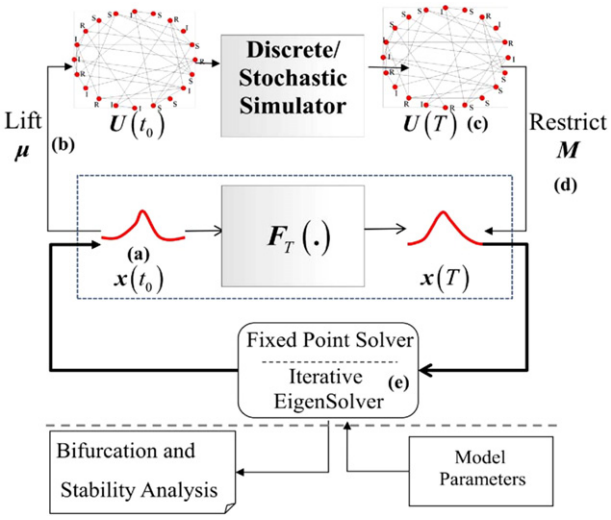

Figure 3. Schematic description of the equation-free approach.

It should be emphasized that such an approach opens the way to tracing bifurcation diagrams and extracting higher-level information acting directly on the detailed simulator. The coarse-grained equilibria can be computed as fixed points of the coarse timestepper

$$\boldsymbol{x}_{\mathrm{eq}} - \boldsymbol{F}(\boldsymbol{x}_{\mathrm{eq}}, \boldsymbol{p}) = 0 \tag{21}$$

via convergence procedures such as Newton–Raphson iteration. In a similar way, the stability of the states can be fully evaluated through numerical estimates of the Jacobian matrix. The coarse-grained unstable branches were here traced by augmenting the system with a pseudo-arc length continuation [38].

5. Results

Our purpose here is to compare the efficiency of the different closure schemes (analytical and numerical) in reproducing the emergent behavior and performing system-level analysis of the above-defined epidemic model. To this end, we will compare single trajectories as well as bifurcation diagrams from full simulations with the corresponding predictions obtained with the various closures.

As an example, figure 4 depicts the evolution of the density of infected individuals $[I]$ in the network for different values of λ. These results were obtained using the original detailed individual-based stochastic model. As can be seen, for relatively large values of this parameter there exists only one coarse-grained steady state which corresponds to a state of high endemicity (figures 4(a) and (b)). The same behavior is observed for even smaller values of the probability ($\lambda = 0.32$, figure 4(c)). By slightly decreasing this parameter though ($\lambda = 0.27$), and depending on the initial condition, another coarse-grained steady state emerges corresponding to a state of low endemicity (figure 4(d)). This behavior is conserved for smaller values of the transition probability ($\lambda = 0.1$, figure 4(e)) until, for extremely low values, the only possible coarse-grained state is a 'disease-free' system (figure 4(f)).

J. Stat. Mech. (2012) P08020

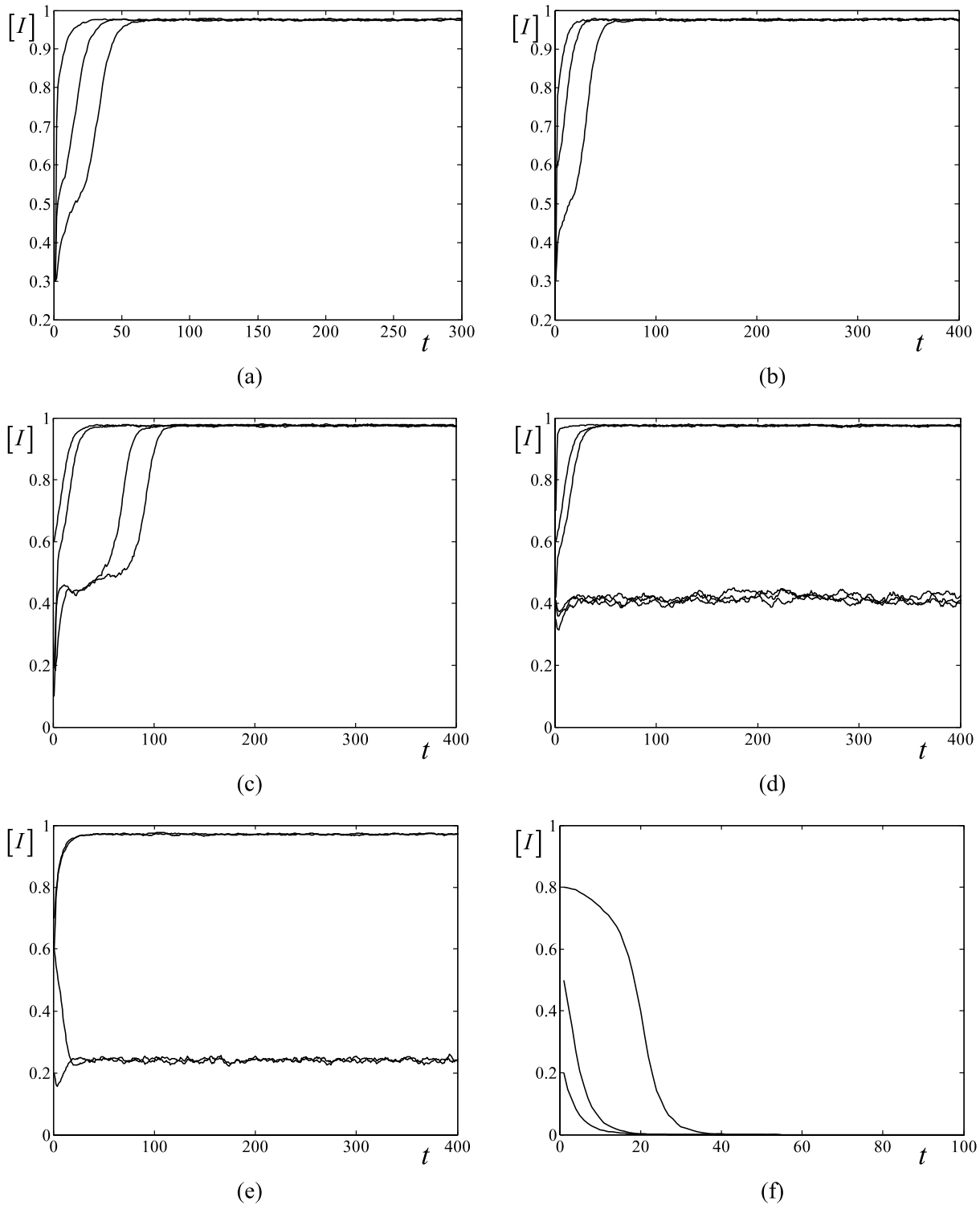

Figure 4. Temporal simulations of the density of infected individuals $[I]$ starting from different initial conditions in the case of the Erdős–Rényi network for values of the probability: (a) $p_{S\to I} = 0.7$, (b) $p_{S\to I} = 0.5$, (c) $p_{S\to I} = 0.32$, (d) $p_{S\to I} = 0.27$, (e) $p_{S\to I} = 0.1$, (f) $p_{S\to I} = 0.01$.

J. Stat. Mech. (2012) P08020

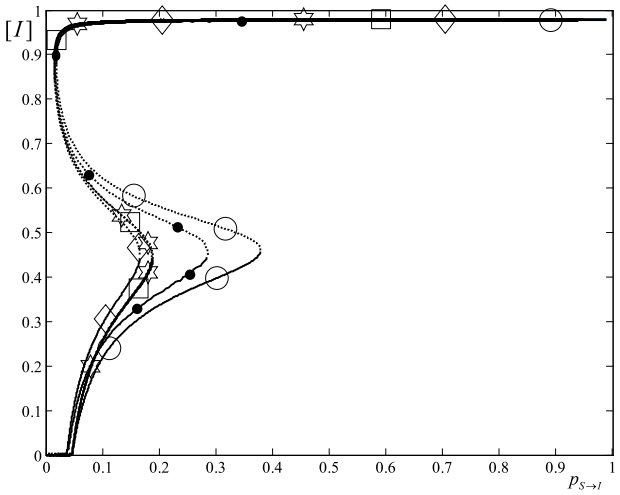

Figure 5. Bifurcation diagrams of the density of infected individuals $[I]$ with respect to the parameter λ in the case of the equation-free approach (dark circles), the mean field approximation (diamonds), the Kirkwood factorization (squares), the Ursell expansion (hexagrams) and the Bethe-type Ansatz (open circles). Solid lines correspond to stable coarse-grained equilibria, while, the dotted lines correspond to unstable ones.

This nonlinear behavior suggests the existence of a bistable region sandwiched between critical points that mark its onset and, according to bifurcation theory, also points towards the existence of intermediate, unstable coarse-grained steady states. The position of the stable steady states and the localization of the bifurcation points can readily be attained through long simulation runs of the full stochastic dynamics. In particular it was found that the disease-free state loses stability at $\lambda \approx 0.038$, giving birth to a branch of stable steady states of low endemicity; this branch in turn loses stability at $\lambda \approx 0.288$; further increase of λ drives the system to a branch of stable steady states of high endemicity, which in turn loses stability for smaller values of λ at $\lambda \approx 0.0165$. The intermediate unstable branch as well as the nature of the transition points are, however, much less trivial to obtain and hence restrict one's knowledge of the system's dynamical properties at the macroscopic scale.

This information can be obtained through the above-mentioned explicit closure schemes or by exploiting the equation-free approach. Figure 5 depicts the coarse-grained bifurcation diagrams derived by the set of equations extracted in each approximation, compared with the one extracted using the proposed computational framework. Note that the equation-free results are obtained by considering only the average densities as the macroscopic variables, i.e. they do not include explicitly high-order moments such as pairs or triplets. The approximation schemes of the epidemic model give a qualitative approximation of the actual emergent dynamics but fail to capture the 'exact' behavior of the individual-based simulator. The equation-free approach, on the other hand, captures the actual behavior. Let us now consider in more detail the behavior of the analytical closure schemes.

Using the analytical closures, the values for the steady states and the exact localization of the bifurcation points appear to be different from those obtained through full

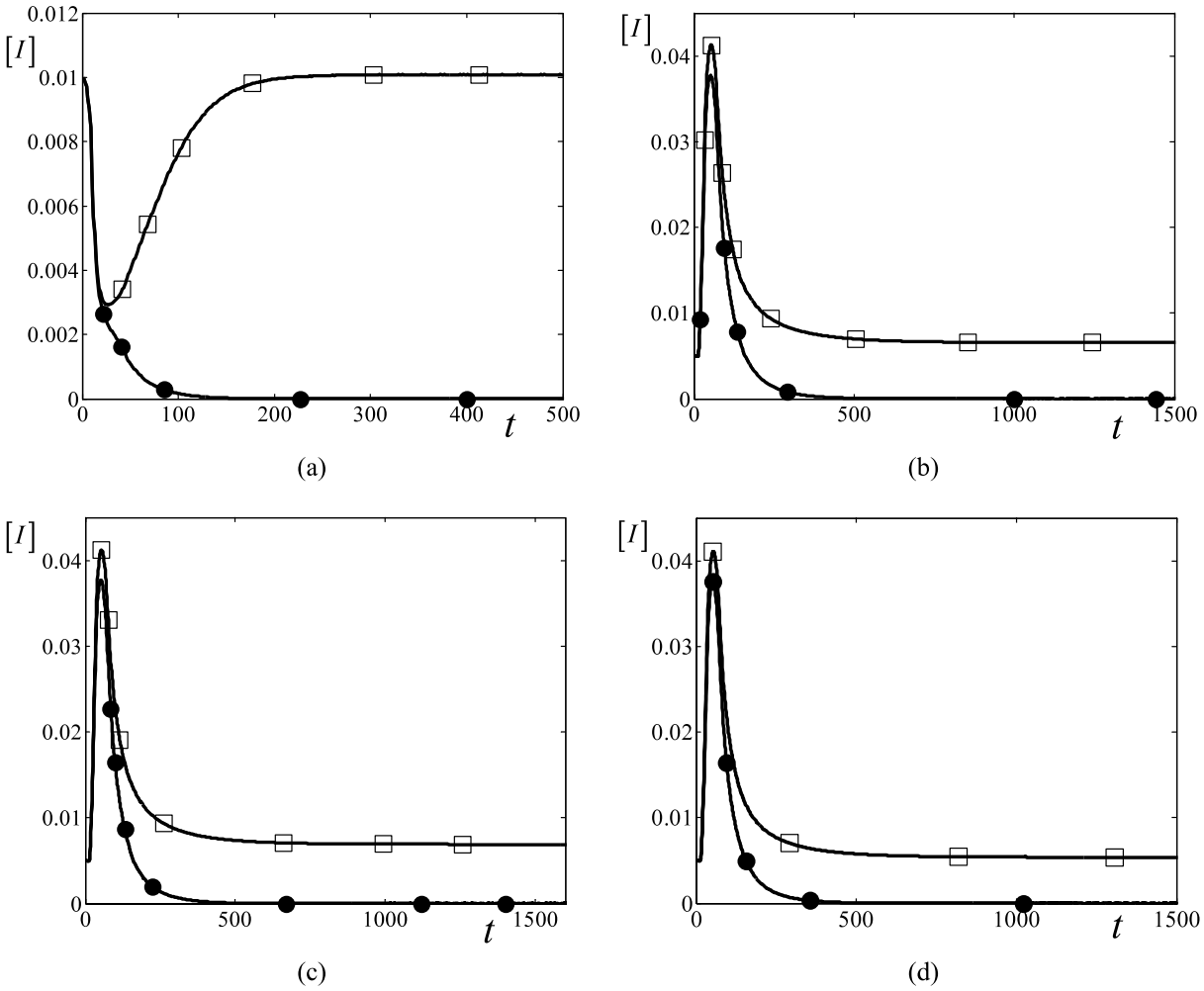

Figure 6. Time evolution of the density of infected individuals $[I]$ in the case of the different approximation schemes of the epidemic model 'near' the critical value that marks the loss of stability of the disease-free state: (a) for the mean field approximation when the value of the parameter is $\lambda = 0.036$ (dark circles) and $\lambda = 0.038$ (squares), (b) the Kirkwood factorization for $\lambda = 0.045$ (dark circles) and $\lambda = 0.047$ (squares), (c) the Ursell expansion for $\lambda = 0.045$ (dark circles) and $\lambda = 0.047$ (squares) and (d) the Bethe-type ansatz for $\lambda = 0.045$ (dark circles) and $\lambda = 0.047$ (squares).

simulations. The different explicit approaches approximate relatively well the critical point which marks the loss of stability of the disease-free state: $\lambda^* \approx 0.037$ in the case of the mean field approach (figure 6(a)), $\lambda^* \approx 0.046$ in the case of the Kirkwood factorization (figure 6(b)), the Ursell expansion (figure 6(c)) and the Bethe-type ansatz (figure 6(d)). One of the two critical points is approximated with a fairly good accuracy, whatever the framework: $\lambda^* \approx 0.015\,19$ in the mean field approximation (figure 7(a)), $\lambda^* \approx 0.015\,46$ in the Kirkwood factorization (figure 7(b)) and in the Ursell expansion (figure 7(c)) and $\lambda^* \approx 0.018\,93$ in the case of the Bethe-type ansatz (figure 7(d)). All these approximations however fail pretty badly in predicting the critical point in which the low-endemic steady

J. Stat. Mech. (2012) P08020

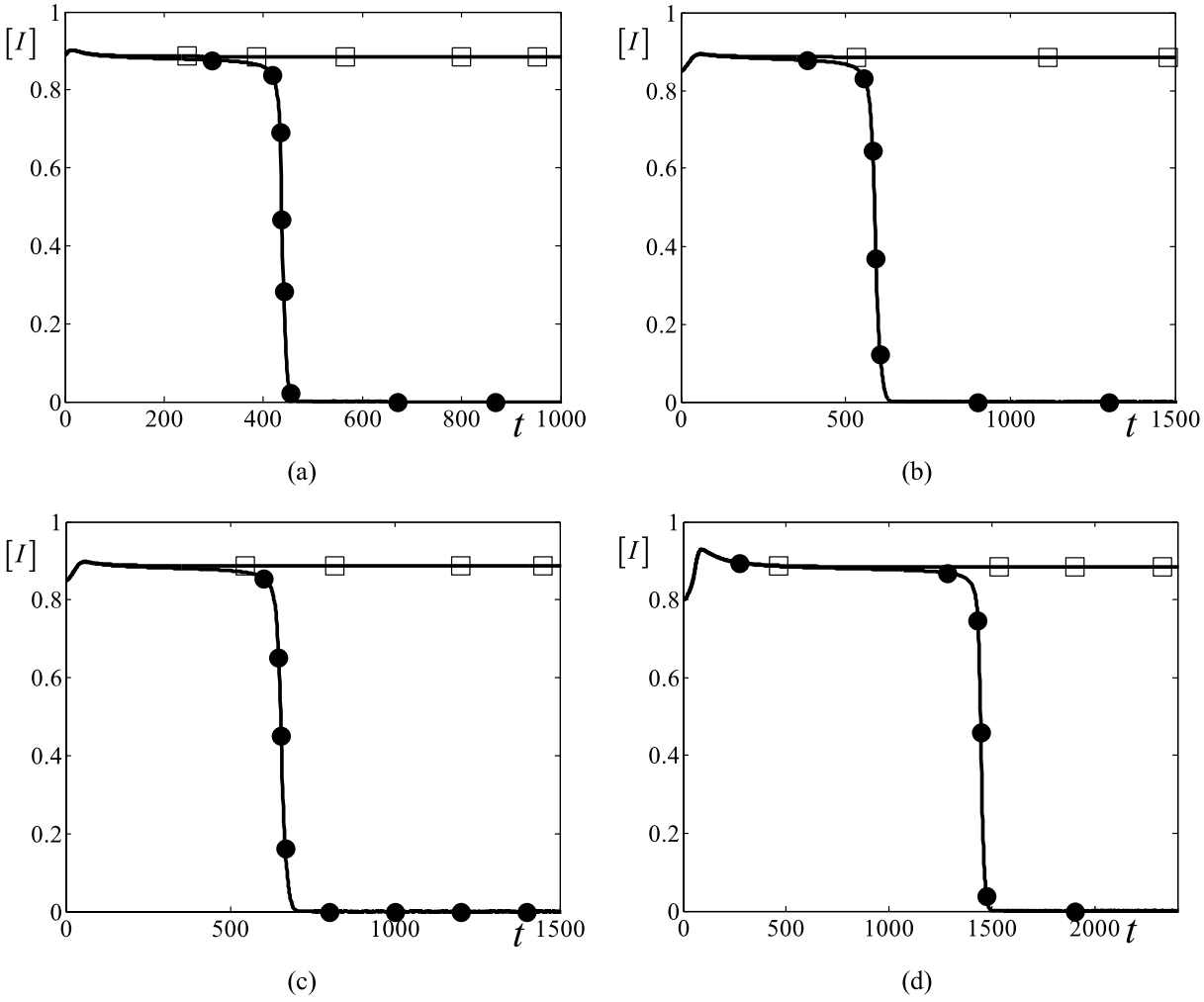

Figure 7. Time evolution of the density of infected individuals $[I]$ in the case of the different approximation schemes of the epidemic model 'near' the critical value that marks the loss of stability of the high-endemic state: (a) for the mean field approximation when the value of the parameter is $\lambda = 0.015\,17$ (dark circles) and $\lambda = 0.015\,22$ (squares), (b) the Kirkwood factorization for $\lambda = 0.015\,43$ (dark circles) and $\lambda = 0.015\,48$ (squares), (c) the Ursell expansion for $\lambda = 0.015\,43$ (circles) and $\lambda = 0.015\,48$ (squares) and (d) the Bethe-type ansatz for $\lambda = 0.018\,9$ (dark circles) and $\lambda = 0.018\,95$ (squares).

state loses stability and the density of infected individuals finally converges to the state of high endemicity: $\lambda^* \approx 0.1662$ in the case of the mean field approximation (figure 8), $\lambda^* \approx 0.1894$ in the Kirkwood factorization (figure 9), $\lambda^* \approx 0.1872$ in the Ursell expansion (figure 10) and $\lambda^* \approx 0.3792$ in the Bethe-type ansatz (figure 11). This casts doubts on the other predictions of these analytical closures, such as those on the nature of the transitions points or the stability of the states. Note, however, that the different approaches seem to agree, in the sense that they all predict the transition points to be two regular turning points marking an interchange of stability between coarse-grained stable (solid lines) and unstable (dotted line) states.

J. Stat. Mech. (2012) P08020

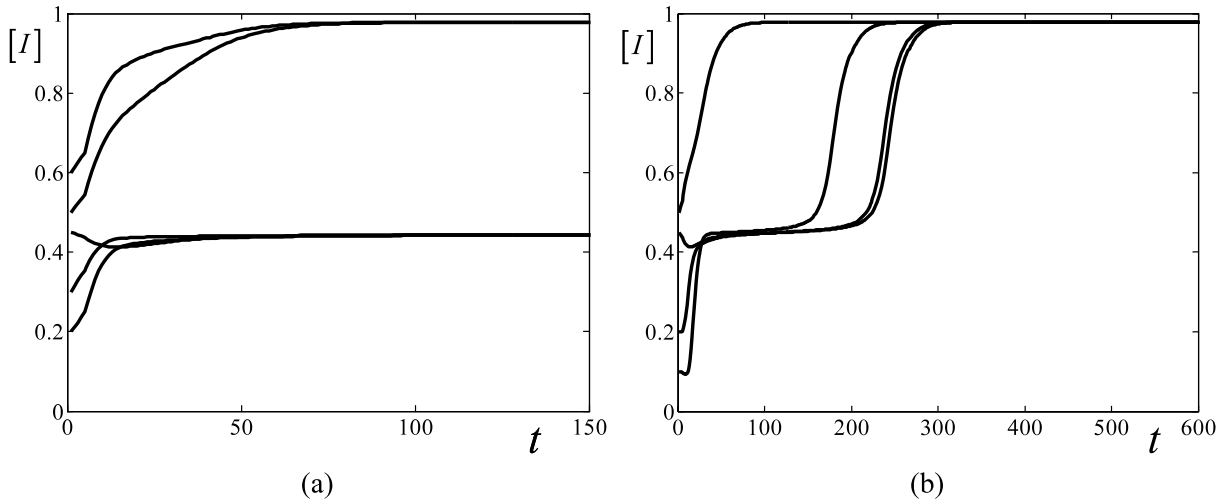

Figure 8. Time evolution of the density of infected individuals $[I]$ starting from different initial conditions in the case of the mean field approximation of the epidemic model 'near' the critical value, $\lambda^* \approx 0.1662$, that marks the loss of stability of the low-endemic state: (a) when the value of the parameter is equal to $\lambda = 0.166$ and (b) when the value of the parameter is equal to $\lambda = 0.1665$.

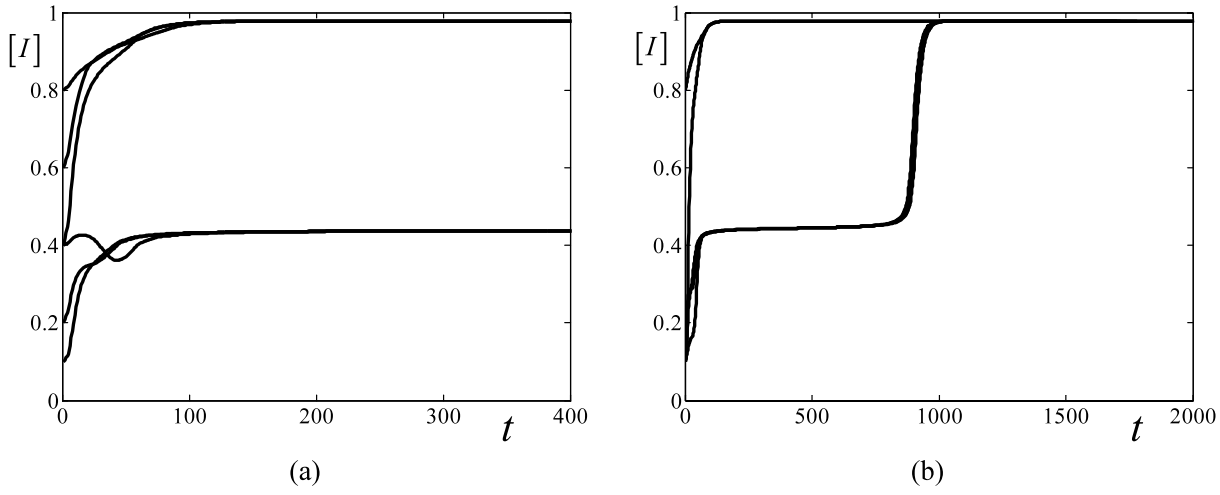

Figure 9. Time evolution of the density of infected individuals $[I]$ starting from different initial conditions in the case of the Kirkwood factorization of the epidemic model 'near' the critical value, $\lambda^* \approx 0.1893$, that marks the loss of stability of the low-endemic state: (a) when the value of the parameter is equal to $\lambda = 0.189$ and (b) when the value of the parameter is equal to $\lambda = 0.1895$.

A detailed version of the bifurcation diagram obtained via the equation-free method is given in figure 12. This diagram (also plotted in figure 5) was extracted by wrapping around the coarse timestepper of the densities ($[I]$ and $[S]$) a Newton–Raphson iteration with a time horizon $T = 7$ and by averaging over 10 000 realizations of the individual-based stochastic simulator. The numerical values for the steady states as well as the localization

J. Stat. Mech. (2012) P08020

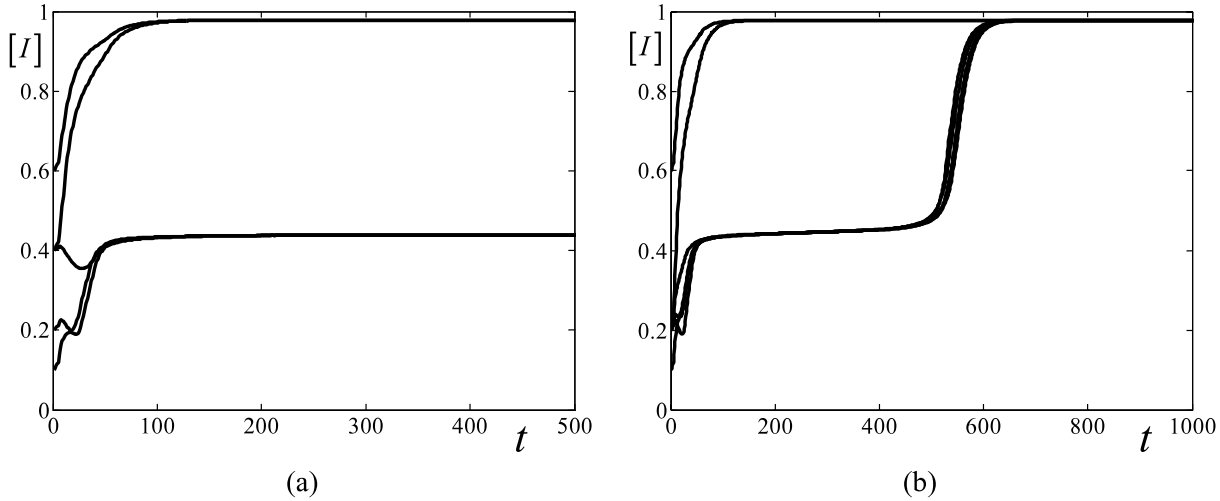

Figure 10. Time evolution of the density of infected individuals $[I]$ starting from different initial conditions in the case of the Ursell expansion of the epidemic model 'near' the critical value, $\lambda^* \approx 0.1872$, that marks the loss of stability of the low-endemic state: (a) when the value of the parameter is equal to $\lambda = 0.187$ and (b) when the value of the parameter is equal to $\lambda = 0.1875$.

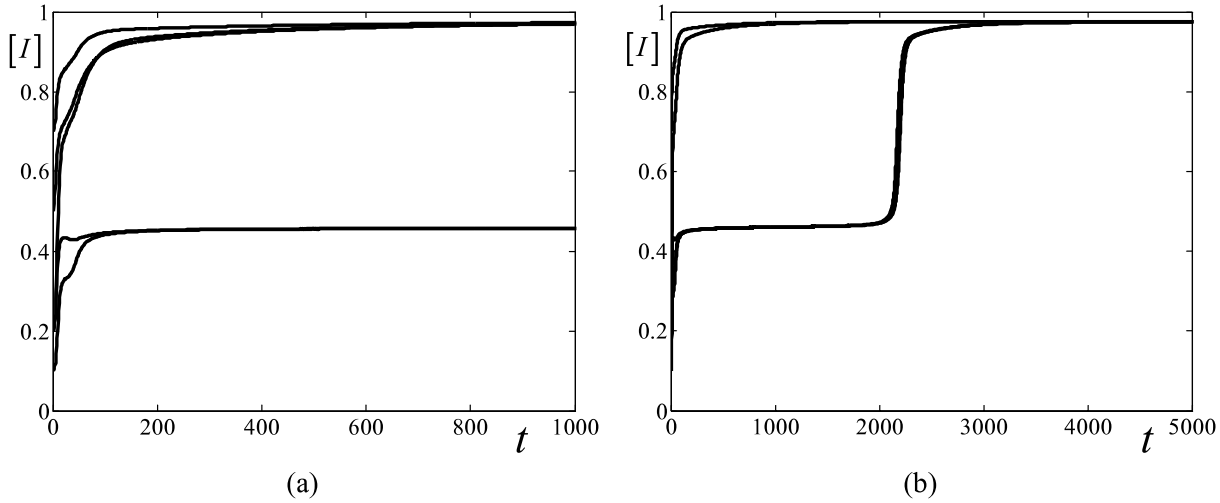

Figure 11. Time evolution of the density of infected individuals $[I]$ starting from different initial conditions in the case of the Bethe-type ansatz of the epidemic model 'near' the critical value, $\lambda^* \approx 0.3792$, that marks the loss of stability of the low-endemic state: (a) when the value of the parameter is equal to $\lambda = 0.379$ and (b) when the value of the parameter is equal to $\lambda = 0.3795$.

of the transition points are in excellent agreement with respect to the detailed individual-based simulations. Just like when using analytical closure relations, the equation-free framework allows the analysis of the nature of the transition points. For example, the inset of figure 12(a) illustrates the algebraically largest (numerically obtained) eigenvalue with respect to the bifurcation parameter. This analysis confirms the results obtained with

J. Stat. Mech. (2012) P08020

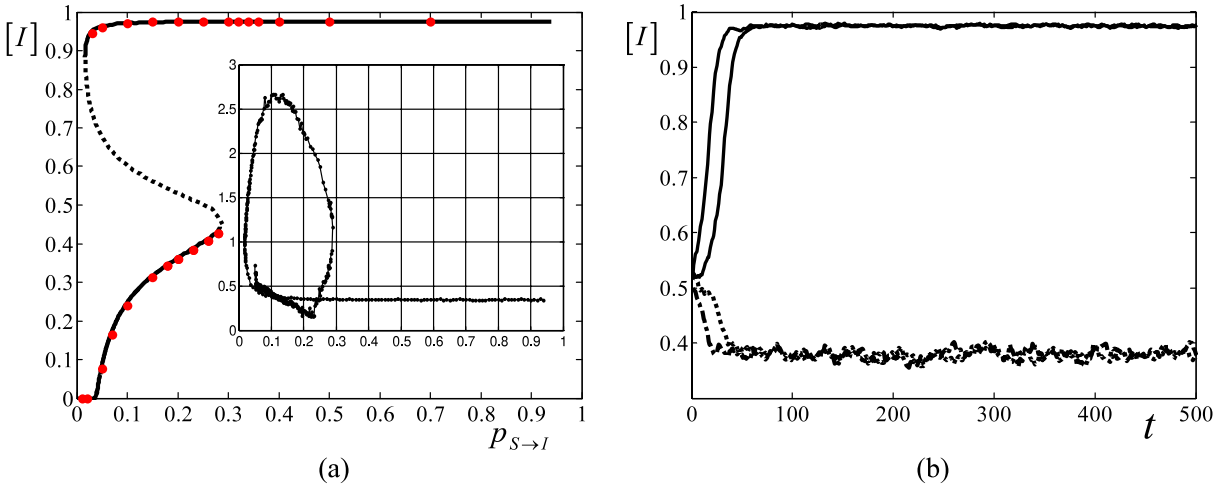

Figure 12. (a) Coarse-grained bifurcation diagram of the density of infected individuals $[I]$ with respect to the probability $p_{S\to I}$ for the Erdős–Rényi network. Solid lines depict the stable coarse-grained steady states while the dotted lines depict the unstable ones. The (red) dots represent the mean values of the density of infected individuals at steady state, for different values of the probability $p_{S\to I}$, extracted by performing long-run temporal simulation of the stochastic dynamics. (b) Temporal simulations of the density of infected individuals, $[I]$ for value of the probability $\lambda = 0.2273$ starting from different initial conditions 'near' the unstable equilibrium as estimated using the equation-free approach ($[I]^{\text{eq}}_{\text{unstable}} \approx 0.5139$).

the other approaches (the critical points are saddle-node bifurcations) but the high level of agreement with the full simulations makes these predictions now much more reliable. The equation-free approach also allows one to precisely localize the position of unstable coarse steady states, as is illustrated in figure 12(b). There, we plot the evolution of the density of infected individuals $[I]$ as obtained from full simulations, when λ is set equal to 0.2273 and the network is initialized 'near' the coarse-grained unstable state predicted by the equation-free approach. These simulations confirm the existence of a separatrix between the two basins of attraction, at exactly this position. The coarse-grained solutions found by the proposed framework thus seem fully consistent with the long-run detailed temporal simulations.

It is relevant to try and understand why the equation-free approach is so efficient in our case. The most surprising is maybe that it is able to correctly characterize the stochastic model, by only incorporating the coarse-grained densities just like the mean field approach, which here completely fails. As stated in section 4, the first step of the equation-free approach is to identify the coarse-grained statistics. The main assumption is that a good coarse-grained macroscopic model exists and closes in terms of a few coarse-grained observables which correspond to some lower-order moments of the underlying microscopic distributions. The fact that the densities alone are enough to reproduce the dynamics points to the aforementioned idea that the higher-order moments rapidly become functionals of these lower ones. In our case it would mean that the first-order moments of the individual-based distribution (the densities of infected, recovered or susceptible individuals) govern the emergent dynamics. This can actually be verified numerically.

J. Stat. Mech. (2012) P08020

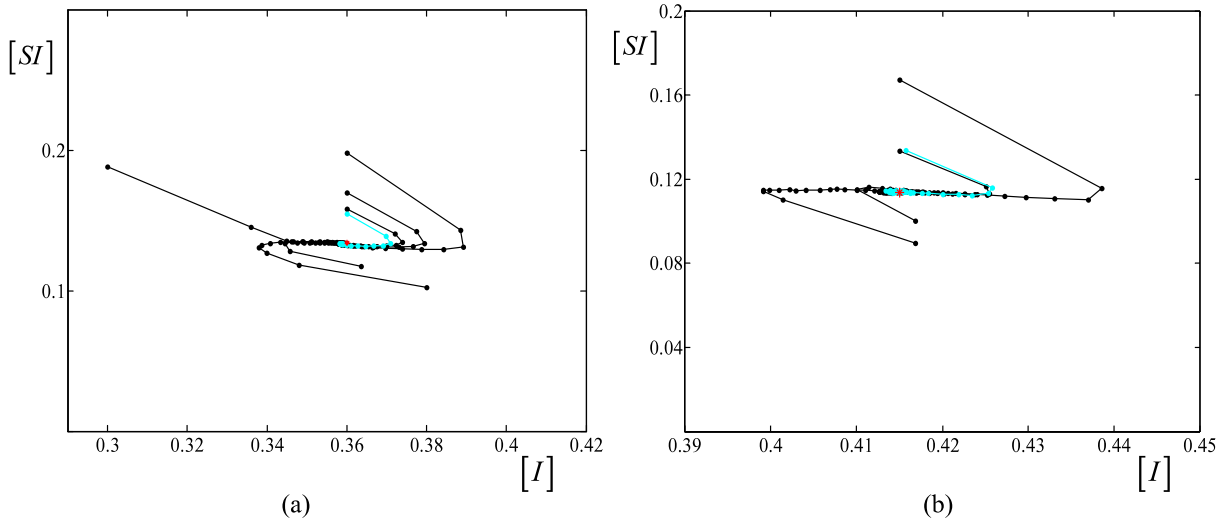

Figure 13. Phase portrait of the density of infected individuals $[I]$ versus the pair $[SI]$ for (a) $\lambda = 0.2$, (b) $\lambda = 0.27$ (close to the turning point) averaged over 1000 realizations. The dynamics are characterized by two stages: an initial 'fast' approach (within 3 or 4 time steps) to a one-dimensional slow manifold which can be parameterized by the density $[I]$ and a slow approach to the coarse-grained stationary state (depicted with a red star) on this slow manifold. The cyan (light) line represents the case where we initialize the system only with the values of the density of Infected and Susceptible (without any Simulated Annealing process).

Figure 13 depicts the phase plane of the density of infected, $[I]$, versus the density of infected connected with susceptible individuals, $[SI]$. In order to create ensembles consistent with the first- and second-order moments we used a Simulated Annealing procedure to initialize the coarse-grained quantities at will [39].

It is important to note here that, while this result indeed confirms the existence of a slaving with respect to the densities only, the corresponding parameterization of the manifold is *not* given by the mean field approximation. This is rather surprising, as the reason usually invoked for the failure of the mean field approach is precisely the impossibility that the dynamics be controlled by the averages only. In other words, it appears that there is indeed a clear-cut separation of time scales between the moments of different order, but that the mean field approximation simply fails in finding the correct expression that connects the moments to each other. Finding the reasons behind the time scale separation, and behind the failure of the mean field approach, is outside the scope of this work but is worth investigating in the future.

Finally, figure 14 illustrates the bifurcation diagrams of the $[SI]$ pair (a) and the $[SIR]$ triple (b), with respect to $p_{S\to I}$ as computed from (i) the actual individual-based simulation, (ii) the explicit closures, and (iii) the equation-free approach (similar results are obtained for any other pair or triple). It is clearly shown that the equation-free approach succeeds pretty well (while the other explicit closures fail) in approximating the actual relation between the lower-order moments (densities) and higher-order moments (pairs and triplets).

J. Stat. Mech. (2012) P08020

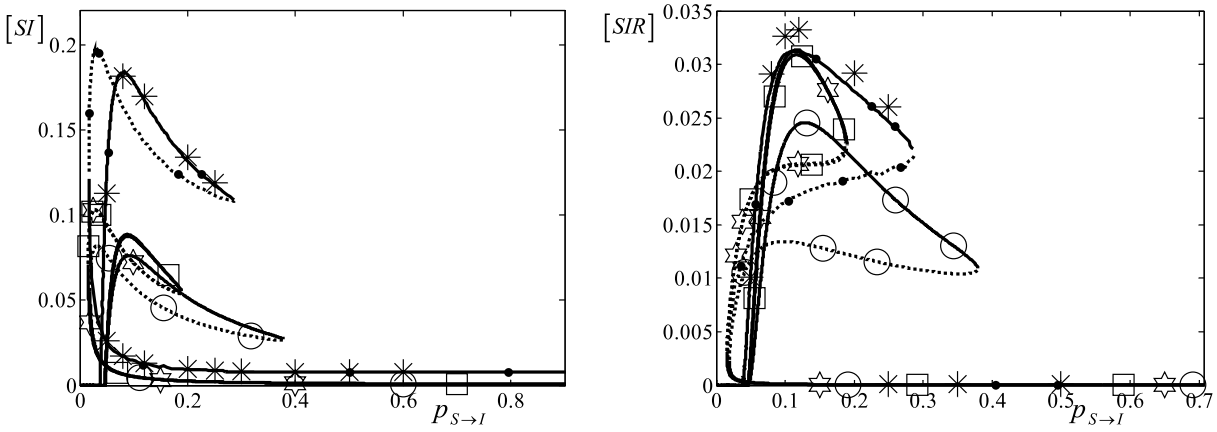

Figure 14. Bifurcation diagrams of (a) the pair $[SI]$ and (b) the triple $[SIR]$, with respect to the probability $p_{S\to I}$ in the case of the equation-free approach (dark circles), the Kirkwood factorization (squares), the Ursell expansion (hexagrams) and the Bethe-type Ansatz (open circles). The actual values as obtained through the temporal simulations of the individual-based simulator are also depicted (stars). Solid lines correspond to stable equilibria, while the dotted lines correspond to unstable ones.

6. Discussion and conclusions

The complexity of individual-based stochastic models evolving on complex networks makes the accurate modeling of the emergent macroscopic behavior a difficult task. Traditionally one tries to extract a master equation, which however can rarely be solved analytically. Instead it is usually solved numerically using transfer matrix techniques, or by performing statistics based on stochastic simulators (such as Gillespie, Kinetic Monte Carlo). Our focus here is however not on the whole probability distribution, but rather on the temporal evolution of some of its low-order moments, such as the density (the first moment) of infected individuals in the network. Unfortunately, extracting these evolution laws from the master equation reveals an infinite-dimensional set of linear equations (in the macroscopic limit), coupling the different moments to each other. One then needs to close, to 'truncate' that hierarchy of equations in order to be able to write down explicitly rate equations for the quantities of interest.

In the case of dynamics on networks, this procedure has traditionally followed two main paths. One involves some 'ad hoc' factorization of higher moments as functionals of the lower ones. This type of approximation actually amounts to assuming a specific form for the inter-particular correlation functions, e.g. the eigenfunctions of the graph-Laplacian can provide a low-dimensional, coarse description of the functions evolving on the network. They can thus be rationalized starting from a systematic expression of the correlations as functions of the moments themselves: this expansion is usually referred to as the Ursell development. For example, the most popular factorization of this type (known as the Kirkwood approximation) is largely inspired by the factorization of the 3-points correlation function used in the equilibrium statistical mechanics of fluids. In

J. Stat. Mech. (2012) P08020

this case, the procedure closes the hierarchy at the level of the second moments. Other types of factorization can also be found in the literature that close the hierarchy at the same order (such as the Bethe-type ansatz that we use here), or can include contributions from the third, fourth, etc moments as well.

Another path consists in closing the hierarchy by assuming the existence of some rapidly evolving higher moments (or combination thereof) so that a quasi-steady state approximation can be used. In effect, this approach also leads to high-order moments being functionals of the lower ones, but here the connection between these variables is made through an inspection of the dynamical equations, and is not based on some 'static' hypothesis on the correlation functions (as above). This procedure is usually very efficient, but is highly model-dependent and is less easy to implement if one seeks to explicitly write down the evolution equations for the moments. Here we exploited the equation-free approach, which rests on such a separation of time scales, but bypasses the need for explicitly extracting the closure relations. This is achieved by treating the detailed simulator as a black-box timestepper of a few coarse-grained observables to estimate the coarse-grained quantities required for continuum numerics. The key assumption of the method is that macroscopic equations do in principle exist, i.e. that fast higher-order moments of the underlying detailed distribution become very quickly functionals of a few lower-order moments. This implies that the emergent dynamics can be described on a slow manifold parameterized by these lower-order moments. For our illustrations, we used a simple SIRS epidemic model evolving on a Erdős–Rényi network. By constructing and comparing the coarse-grained bifurcation diagrams obtained with different closure schemes with the one computed with the equation-free approach, we showed that this approach is able to catch the actual emergent dynamical behavior, outperforming all the other explicit schemes.

The success of the equation-free approach in the system under consideration is a strong sign that a clear separation of time scales exists between the densities and higher-order moments. This implies that the emergent dynamics could, in principle, be written as a set of evolution equations only involving the densities. This latter property is usually seen as a sign that the traditional mean field approach is a relevant approximation. However, the parameterization of higher moments with respect to these lower ones is here not the mean field one. One could wonder what special properties of the system dynamics are behind this time scale separation, and why they do not lead to a mean field type of emergent behavior. We believe this is a question of general interest: knowing that a whole class of stochastic epidemics models can be described only in terms of densities would reveal fundamental information for the study of these systems. We thus plan on using the equation-free approach on more complex heterogeneous networks to assess the generality of this result. In such cases the interplay of the heterogeneous topology and emergent model dynamics renders the systematic derivation of closures an overwhelmingly difficult task. For example, for correlated structures, such as small-world topologies, one should also take into account characteristics such as assortativity, clustering, path length and betweenness. In parallel, we will also be seeking the origin of this behavior in the peculiar form of transition probabilities for lattice systems, which determine the spectrum of time scales in such systems.

J. Stat. Mech. (2012) P08020

Appendix

A.1. Evolution equations using Ursell expansion

$$
\begin{aligned}
\frac{\mathrm{d}[I]}{\mathrm{d}t} &= \lambda z[SI] - \delta[I] \\
\frac{\mathrm{d}[R]}{\mathrm{d}t} &= \delta[I] - \gamma[R] \\
\frac{\mathrm{d}[SR]}{\mathrm{d}t} &= \delta[SI] + \gamma([R] - [RI] - 2[SR]) - (z-1) \\
&\quad \times \lambda([I][SR] + [R][SI] - [I][R](1 - [I] - [R])) \\
\frac{\mathrm{d}[RI]}{\mathrm{d}t} &= -(2\delta + \gamma)[RI] + \delta([I] - [SI]) \\
&\quad + (z-1)\lambda([I][SR] + [R][SI] - [I][R](1 - [I] - [R])) \\
\frac{\mathrm{d}[SI]}{\mathrm{d}t} &= \gamma[RI] - (\lambda + \delta)[SI] + (z-1)\lambda([SI](1 - [I] - [R]) + [I] \\
&\quad \times (1 - [I] - [R] - [SR] - [SI]) - [I](1 - [I] - [R])^2) \\
&\quad - (z-1)\lambda(2[I][SI] - [I]^2(1 - [I] - [R])).
\end{aligned}
\tag{A.1}
$$

A.2. Evolution equations using the Bethe-type Ansatz

$$
\begin{aligned}
\frac{\mathrm{d}[I]}{\mathrm{d}t} &= \lambda z[SI] - \delta[I] \\
\frac{\mathrm{d}[R]}{\mathrm{d}t} &= \delta[I] - \gamma[R] \\
\frac{\mathrm{d}[SR]}{\mathrm{d}t} &= \delta[SI] + \gamma([R] - [RI] - 2[SR]) - (z-1)\lambda([R][SI]) \\
\frac{\mathrm{d}[RI]}{\mathrm{d}t} &= -(2\delta + \gamma)[RI] + \delta([I] - [SI]) + (z-1)\lambda([R][SI]) \\
\frac{\mathrm{d}[SI]}{\mathrm{d}t} &= \gamma[RI] - (\lambda + \delta)[SI] + (z-1)\lambda[SI](1 - [R] - 2[I]).
\end{aligned}
\tag{A.2}
$$

References

[1] Eubank S, 2004 *Nature* **429** 180
[2] Ferguson N M *et al,* 2005 *Nature* **437** 209
[3] Burke D *et al,* 2006 *Acad. Emerg. Med.* **13** 1142
[4] Longini I *et al,* 2007 *Int. J. Infectious Diseases* **11** 98
[5] Doedel E and Tuckerman L S, 2005 *Numerical Methods for Bifurcation Problems and Large-Scale Dynamical Systems* (New York: Springer)
[6] Dhooge A *et al,* 2003 *ACM Trans. Math. Software* **29** 141
[7] Doedel E J *et al,* 2005 *Int. J. Bifurcation Chaos* **15** 841
[8] Matsuda H, 1992 *Prog. Theor. Phys.* **88** 1035
[9] Keeling M J, 1999 *Proc. R. Soc.* B **266** 859
[10] Keeling M J and Eames K T, 2005 *J. R. Soc. Interface* **2** 295
[11] Simon P L *et al,* 2001 *J. Math. Biol.* **62** 479
[12] Keeling M J and Ross J V, 2008 *J. R. Soc. Interface* **5** 171
[13] Taylor M *et al,* 2012 *J. Math. Biol.* **64** 1021

doi:10.1088/1742-5468/2012/08/P08020

J. Stat. Mech. (2012) P08020

[14] Hausken K and Moxnes J F, 2010 *Math. Comput. Modelling Dyn. Syst.* **16** 555
[15] Murrel D J *et al,* 2004 *J. Theor. Biol.* **229** 421
[16] Bauch C T, 2004 *Math. Biosci.* **198** 217
[17] Filipe J A N and Gibson G J, 2001 *Bull. Math. Biol.* **63** 603
[18] Hiebeler D, 2006 *Bull. Math. Biol.* **66** 1315
[19] Brown D H and Bolker B M, 2004 *Bull. Math. Biol.* **66** 341
[20] Rogers T, 2011 *J. Stat. Mech.* P05007
[21] Hauerta C and Szabo G, 2005 *Am. J. Phys.* **73** 405
[22] Makeev A G *et al,* 2002 *J. Chem. Phys.* **116** 10083
[23] Kevrekidis I G *et al,* 2003 *Commun. Math. Sci.* **1** 715
[24] Siettos C I *et al,* 2003 *J. Chem. Phys.* **118** 10149
[25] Siettos C I *et al,* 2003 *AIChE J.* **49** 1922
[26] Kevrekidis I G *et al,* 2004 *AICHE J.* **50** 1346
[27] Cisternas J *et al,* 2006 *Proc. R. Soc. Lond.* A **460** 2761
[28] Siettos C I, 2006 *Comput. Chem. Eng.* **30** 1632
[29] Kirkwood J G and Boggs E M, 1942 *J. Chem. Phys.* **10** 394
[30] Abad E *et al,* 2001 *Phys. Rev.* E **63** 041102
[31] Prakash S and Nicolis G, 1996 *J. Stat. Phys.* **82** 297
[32] Prakash S and Nicolis G, 1997 *J. Stat. Phys.* **86** 1289
[33] Erdős P and Rényi A, 1959 *Pub. Math.* **6** 290
[34] Joo J and Lebovitz J L, 2004 *Phys. Rev.* E **70** 036114
[35] Levin S and Durret R, 1996 *Trans. R. Soc. London* **351** 1615
[36] Surda A and Karasova I, 1991 *Surf. Sci.* **109** 605
[37] Fenichel N, 1979 *J. Differ. Equat.* **31** 53
[38] Kelley C T, 1995 *Iterative Methods for Optimization* (Philadelphia, PA: SIAM)
[39] Siettos C I, 2010 *Appl. Math. Comput.* **218** 324

J. Stat. Mech. (2012) P08020